I.S. Petrik [1], G.V. Krylova [3], O.O. Kelyp [1], L.V. Lutsenko [2], N.P. Smirnova [1], L.P. Oleksenko [2]

XPS AND TPR STUDY OF SOL-GEL DERIVED M/TiO$_2$ POWDERS (M=Co, Cu, Mn, Ni)

[1] *Chuiko Institute of Surface Chemistry of National Academy of Sciences of Ukraine*
17 General Naumov Str., Kyiv, 03164, Ukraine, E-mail: irinapetrik@ukr.net
[2] *Taras Shevchenko National University of Kyiv*
60 Volodymyrska Str., Kyiv, 01601, Ukraine
[3] *University of Notre Dame*
132 Nieuwland Science Hall, Notre Dame, IN, 46556, USA

Produced by templated sol-gel method mesoporous nanosized titania powders modified with 3d-metal ions have been characterized by XPS and TPR methods. Metal species formed on the titania surface were investigated. The TPR analysis showed that reduction behaviors of the M^{n+}/TiO_2 were strongly affected by the synthesis method, preparation conditions and interactions between the dopant metal and TiO$_2$ matrix. It was found that Ti–O–M– bonds formation during sol-gel synthesis with applying nonionic triblock copolymer Pluronic P123 as organic template and calcination at 550 °C promoted high-dispersion states of doped 5 % metals. The XPS and TPR showing dopants exist as divalent and trivalent ions for M^{n+}/TiO_2, where M=Co, Ni, Mn, and as monovalent and divalent ions in the case of Cu/TiO$_2$.

***Keywords**: mesoporous M^{n+}/TiO_2 powders, Co^{n+}, Ni^{n+}, Mn^{n+} and Cu^{n+} transition metals, XPS, H$_2$–TPR*

INTRODUCTION

Modification of TiO$_2$ for improving its photocatalytic activity is still of vital importance in both theoretical and applied fields. For example, doping of 3*d*-metals on titania surface was studied [1–3]. Several powdered semiconductors were reported to be effective for photocatalytic degradation of dyes, cyanide, pesticide, chloro-organic compounds, hazardous Cr(IV) ions photoreduction, drinking water denitrification [4–9]. However, there is still an urgent need to produce highly active photocatalysts with developed porous structure and high surface area. Recently, we discovered that Co, Ni, Mn and Cu doped TiO$_2$ are a group of active catalysts for UV light induced photoreduction of NO$_2$ in aqueous solution selectively to N$_2$ avoiding of producing nitrate and ammonia as main nitrogen-containing products [10]. The photoactivity of 3*d*-metal doped TiO$_2$ was greatly affected by the state of metal, that is, the crystal size and the reduction degree.

Solid catalysts with high specific surface area, high homogeneity, and controlled redox properties are important in catalytic converters. Chemical and physical properties of solid catalysts depend mainly on the procedures and conditions of preparation. It is known that the Co/TiO$_2$ catalyst is considered to have a strong metal support interaction and shows high activity in CO hydrogenation [11–14]. This interaction is an important factor used for determining the properties of M^{n+}/TiO$_2$ catalyst such as dispersion and reduction behavior of metal species. The main interest in the studies of this kind of catalysts is the identification of nature of the 3d metal species and verification of their relation with its activity in the catalytic and photocatalytic processes. In our previous papers [10, 15, 16] photocatalytic denitrification of water and electrochemical reduction of oxygen using M^{n+}/TiO$_2$ powders and films as catalyst were investigated. Some peculiarities of these redox processes can be explained as a result of coexistence of dopant ions in multivalent states.

In this paper physicochemical properties of mesoporous powders of titanium dioxide modified with transition metal ions (cobalt, nickel, manganese and copper) were investigated by XPS and H$_2$-TPR methods.

EXPERIMENTAL

Mesoporous TiO$_2$, Co^{n+}/TiO$_2$, Ni^{n+}/TiO$_2$, Mn^{n+}/TiO$_2$ and Cu^{n+}/TiO$_2$ powders were

synthesized via templated sol-gel method according to [17] using Ti(OiPr)$_4$, CuSO$_4$·5H$_2$O, Co(CH$_3$COO)$_2$·4H$_2$O, Ni(HCOO)$_2$·2H$_2$O, MnCl$_2$·4H$_2$O as titania and $3d$-metal sources, Pluronic P123 as template and acetylacetone as complexing agent. The molar ratios of the components were as follow: Pluronic P123: acetylacetone : HNO$_3$: Ti(OiPr)$_4$ = 0.1 : 1 : 2 : 2. After gelation and gel ripening, it was dried in air at room temperature for 2 h. Then the dried powders were calcined at 400 °C. P123 burns out at these temperatures and this process should be carefully carried out for keeping the ordered porous structure of the oxide powder.

The electronic structure of the sol-gel powder surface was explored by X-ray photoelectron spectroscopy (XPS) by a electron spectrometer (E Mg$K\alpha$ =1253.6 eV, $P = 10^{-7}$ Pa) with a PHOIBOS-100 energy analyzer SPECS (USA). The spectra of $3d$-metal levels were decomposed into peak couples with parameters of spin–orbit separation ΔE_p ($3d_{3/2} - 3d_{5/2}$) = 6.0 eV and ratio of intensities was I $3d_{3/2}/3d_{5/2}$ = 0.66. Full width at half maximum height (FWHM) was 1.0 eV. The

decomposition was carried out by Gauss–Newton method, the area of peaks were determined after subtraction of the background by Shirley method.

Temperature programmed reduction by hydrogen (TPR) of the samples was carried out using a gas mixture 10 % H$_2$/Ar as reducing agent (flow rate = 60 cm^3/min). The sample (0.25 g) was inserted in a quartz tube and treated in a helium flow at 350 °C for 1 h and cooled to ambient temperature. Then the sample was heated at a rate of 10 °C/min up to 800 °C in the reducing mixture. The hydrogen consumption was measured with a thermal conductivity detector.

RESULTS AND DISCUSSION

As we reported previously [16], after calcination at 450 °C XRD patterns of M/TiO$_2$ powders showed the anatase nanocrystalline phase formation. The average size of crystallites varying from 8 to 20 nm was determined using Sherrer equation applied to the most intensive peak. Particle sizes evaluated from TEM images of M^{n+}/TiO$_2$ powders (Fig. 1, a-d) coincides with XRD data.

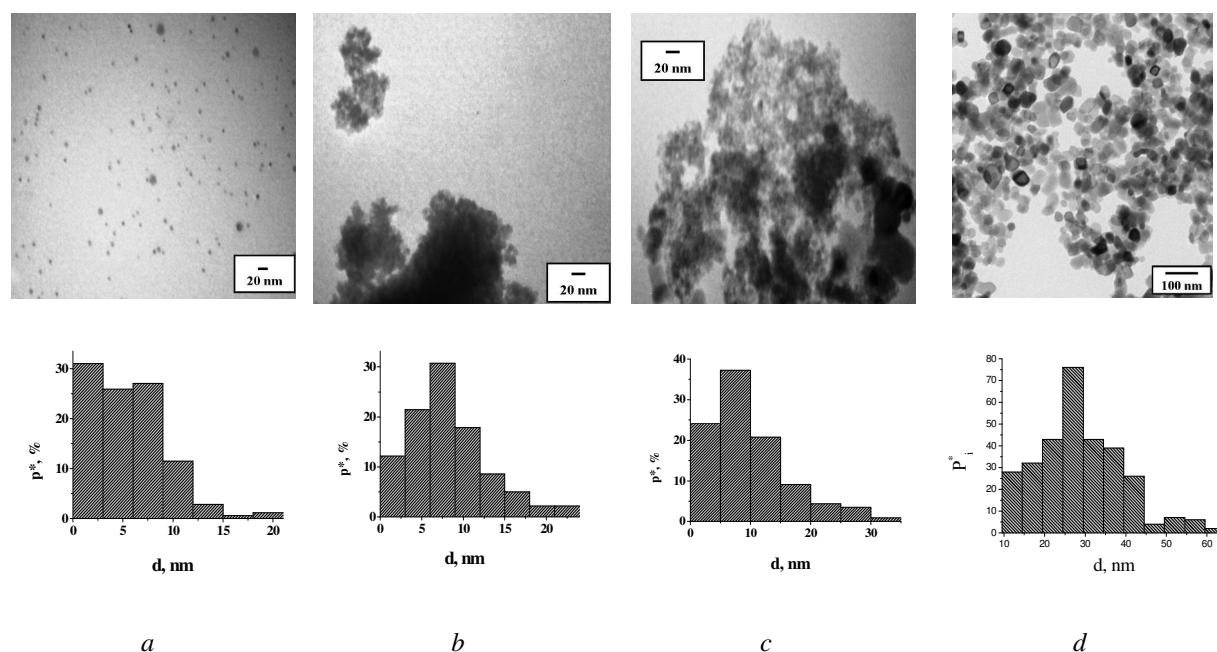**Fig. 1.** TEM images and the histograms of the anatase crystal size distributions for Co^{n+}/TiO$_2$ (a) Ni^{n+}/TiO$_2$ (b), Mn^{n+}/TiO$_2$ (c) and Cu^{n+}/TiO$_2$ (d) powders with dopant concentration 1 %

Investigation of the adsorption-desorption isotherms of nitrogen at –196 °C and the pore size distribution for the powders calcined at 450 °C showed that a mesoporous structure with an average pore size of 2.5–6 nm with specific surface

(S_{BET}) from 147 (pure TiO$_2$) to 224 m^2/g for manganese samples was formed.

The characteristic bands of Co^{2+} and Co^{3+} in octahedral and tetrahedral oxygen environment registered in diffuse reflectance spectra [17]

indicated the formation of Co$_3$O$_4$ spinel phase. Crystallization of M/TiO$_2$ powders after heat treatment at 650 °C led to appearance of absorption bands belonging to Ni^{2+} or Mn^{3+} ions in an octahedral environment. XPS analysis was carried out to determine the chemical and electronic structure of formed nanoparticles and the valence states of selected elements.

Electronic structure of M/TiO$_2$ powders studied by XPS. The XPS result of the undoped TiO$_2$ shows the binding energy (BE) of Ti2$p_{3/2}$ 458.4 eV, which corresponds to BE for pure TiO$_2$ [18]. For Mn/TiO$_2$ a shift to lower BE is observed. This shift can be associated with formation of Ti–O–Co and Ti–O–Mn bonds. In the case of Ni-doped titania Ti2$p_{3/2}$ BE shifts to higher values as compared with undoped TiO$_2$. In accordance with [18, 19], a BE 459.5 eV is an evidence of tetrahedrally coordinated titanium ions in titania lattice, whereas a BE of Ti2$p_{3/2}$ 458.5 eV concerns octahedrally surrounded titanium ions. Since the high-energy shift of Ti2$p_{3/2}$ could be related with change in coordination from octahedral to tetrahedral, the obtained results can point at change in coordination number at forming of Ti–O–Ni bond.

The XPS spectra of O1s region for the M^{n+}/TiO$_2$ systems are presented by three peaks revealing different oxygen states. The peak positioned at 528.1–530.6 eV corresponds to O^{2-} anions in titania lattice, the peak positioned at 530.6–532.3 eV corresponds to oxygen in surface-active OH-groups, and the peak positioned at 532.2–533.7 – to adsorbed on the surface oxygen-containing anions of acid residues [20, 21].

The XPS spectra of 2$p_{3/2}$ region for Co, Ni, Mn and Cu of the M^{n+}/TiO$_2$ samples are collected in Fig. 2. It is seen that Co2$p_{3/2}$ exhibits a principal peak with a shoulder and a strong shake-up satellite (Fig. 2 *a*). The peak with the shoulder may be deconvoluted into two components: 780.3 eV (more intense peak) and 781.6 eV (less intense peak). Absence of photoelectron peaks with BE below 780 eV is indicative of Co^0 absence [22], so cobalt in the Co/TiO$_2$ exists as oxide species. It is commonly recognized that in identifying Co species the satellite structure plays the main role to discern Co^{2+} [23, 24]. The intense satellite observed in the Co2$p_{3/2}$ XPS (Fig. 2 *c*) implies a high contribution of divalent cobalt. Accordingly to [25–27], the peak appearing at 780.3 eV is likely may be assigned to Co$_3$O$_4$ species and the peak appearing at 781.6 eV – to highly dispersed Co^{2+}

species, near to isolated divalent cobalt cations [28, 29]. It is in agreement with broadened satellite structure shape, pointing at the satellite origin from different Co^{2+} type species. Co$_3$O$_4$ is known to have tetrahedral Co^{2+} ions and octahedral Co^{3+} ions [30] and the DRS results received earlier [17] showed the presence of the tetrahedral Co^{2+} and octahedral Co^{2+} ions in the Co/TiO$_2$. The significant intensity of satellite prevailing over the intensity of either of the peaks centered at 780.3 and 781.6 eV is also consistent with this interpretation assumption. Taking into account the XPS result and DRS data [17], we can conclude that cobalt on the titania surface exists in Co$_3$O$_4$ (containing Co^{2+} and Co^{3+} ions), CoO, and CoTiO$_3$ species.

The Ni2$p_{3/2}$ XPS spectrum of Ni-doped TiO$_2$ (Fig. 2 *c*) shows a peak located at 856.0 eV with a distinct shake-up satellite at 6.5 eV higher BE values. The binding energies for nanosized nickel oxide species between 855.3 and 856.7 eV were found to be typical of Ni-doped systems, in particular for Ni/TiO$_2$ [31, 32], the BE shifting to higher values with increasing TiO$_2$ content. This BE is more close to that of Ni2$p_{3/2}$ in Ni$_2$O$_3$ and Ni(OH)$_2$ (Ni^{2+}–compounds with ionic type of bond) than in NiO [32, 33]. Consequently, it can be speculated that nanosized Ti–Ni–O contains Ni$^{2+\delta}$ species, *i.e.* Ni^{3+} ions along with Ni^{2+}ions, and these Ni^{2+} ions are highly dispersed to be considered as isolated ions with decreased electron density (the cations of the titanates) rather than those of bulk oxide.

The XPS spectrum of the Mn-doped TiO$_2$ (Fig. 2 *c*) contains two peaks corresponding to Mn2$p_{3/2}$, attributable to Mn^{2+} at 639.6 eV and to Mn^{3+} at 641.6 eV, and a satellite feature at about 646.0 eV due to Mn^{2+} ions. These BE values are similar to those of corresponding bulk manganese oxides [34], thereby indicating the presence of manganese as oxide-type species.

Fig. 2 *c* shows Cu2$p_{3/2}$ XPS spectrum of the Cu/TiO$_2$. The peaks at 931.7 and 933.3 eV confirm the presence of Cu$^+$ and Cu^{2+} in the Cu-doped TiO$_2$ crystal lattice. Ti^{4+} was successfully deconvoluted from the Ti2p BE for 0 and 5 % Cu-doped TiO$_2$. Ti^{3+} peaks can also be found in the spectrum for the Cu/TiO$_2$. These peaks are indicative of TiO$_2$ and Ti$_2$O$_3$ or Cu$_2$TiO$_3$ and Cu$_3$TiO$_4$. The reduction of Ti^{4+} into Ti^{3+} may be attributed to the presence of Cu species in the TiO$_2$. Additionally, the formal charge generated from the substitution of Cu^{2+} by Cu$^+$ can also be compensated via the

_____

transformation of Ti^{4+} into Ti^{3+}. Oxygen vacancies in the Cu-doped TiO_2 structure may also cause the reduction of Ti^{4+} into Ti^{3+}.

Table 1. The binding energy of core electrons for synthesized M^{n+}/TiO_2 powders

| Sample | The value of the binding energy, eV | | |
| | Ti2$p_{3/2}$ | O1$s_{1/2}$ | |
		Ti–OH	Ti–O–Ti
TiO_2	458.4	531.5	529.7
5 % Co/TiO_2	458.1	531.8	529.3
5 % Ni/TiO_2	459.6	532.3	530.6
5 % Mn/TiO_2	457.3, 458.2	530.6	528.1
5 % Cu/TiO_2	456.4, 458.2, 459.3	531.8	528.5

TPR study of M/TiO$_2$ (M - Co, Ni, Mn, Cu). Temperature-programmed reduction (TPR) was performed to investigate the reducibility of the titania doped with 3d metal ions. The results of the H_2-TPR experiments are presented in Fig. 3. It is seen that the unsupported TiO_2 is characterized by a weak reduction behavior (Fig. 3 *a*), exhibiting a H_2 consumption of low-intensity in region 300–800 °C.

The profile of the Co/TiO_2 shows weak hydrogen consumption up to 400 °C, and a predominant consumption is observed at region 400–800 °C, revealing two distinct reduction regions. Reduction behavior of Co_3O_4 is controversial in the literature, some authors observed a single step for the Co_3O_4 reduction [28, 36], while many others reported about a two-step process, involving with CoO in the reduction [24, 30, 37, 38]. The two-step reduction process consideration supposes that the ratio of the low-temperature peak corresponding to $Co_3O_4 + H_2 \rightarrow 3CoO + H_2O$ reaction to the high-temperature peak corresponding to $CoO + H_2 \rightarrow Co + H_2O$ reaction, should be 1:3 theoretically. But, the profile of the Co/TiO_2 obtained by sol-gel technique and calcinated at 550 °C doesn't confirm this ratio. Thus, the single-step reduction of Co_3O_4 can be proposed, the corresponding peak is centered at 500 °C. High-temperature peak is likely to belong to reduction Co^{2+} particles strongly bound to the support. This is consistent with the XPS data and the DRS results received earlier [17], which indicate the Co^{2+} species along with the Co_3O_4 species.

It should be noted that the reduction peaks for the Co/TiO_2 is shifted to high temperatures. Since the shift of the cobalt reduction peaks to higher temperatures demonstrates an intensity of the cobalt/support interaction, this shift can be explained due to a strong interaction between cobalt and TiO_2. It is known that the interaction increases with a higher dispersion of cobalt on the support surface [36], and at low-loading cobalt the titania has a tendency to stabilize CoO and to resist reduction [38]. Therefore, reduction behavior of cobalt oxide species in TiO_2 doped with small cobalt amounts is strongly affected by supports [24]. The presence of highly dispersed $CoTiO_3$ and/or CoO in addition to Co_3O_4 species was reported also in [39].

From Fig. 3 *c* it can be seen that the TPR profile of the Ni/TiO_2 powder contains two distinct peaks of hydrogen consumption corresponding to different reducible species. The reduction peak of lower intensity with a maximum at 210 °C can be assigned to a reduction of Ni_2O_3 to NiO [31] and nickel ions with formal oxidation number higher than +2. The intense reduction peak with a maximum at 460 °C is attributed to reduction of NiO species resulted from the Ni_2O_3 and of NiO interacted with TiO_2. Doped nickel oxide species usually possess higher reduction temperatures than those of pure oxides due to interaction of nickel with support. Owing to the interaction of nickel with TiO_2, NiO reduces at higher temperatures as compared with free NiO which normally reduces at 285–305 °C [40].

The position and form of reduction peak for dispersed NiO depends on method of preparation, composition and calcination conditions of samples, since these factors cause to different nickel disperse states, sizes of nickel oxide particles and interaction degrees with TiO_2, resulting in variable reducibility of nickel-containing particles. It is known [31, 32], that reduction of nanosized NiO in composite systems Ni–Ti–O occurs at temperatures from 300 to 600 °C depending on the degree of bonding with the surface and accessibility of nickel to be reduced.

Hydrogen consumption at 300–400 °C is assumed to correspond to reduction of bulk NiO on TiO_2 surface, and hydrogen consumption at the temperatures above 400 °C is assigned to NiO significantly bonded with titanium dioxide [31]. Thus the 5 % Ni/TiO_2 is likely to interact at the average degree with the support. An appearance of insignificant H_2 consumption observed at about 600 °C is probably due to reduction of spinel $NiTiO_2$, whith characteristic reduction at 550 °C

[40]. Fig. 3 *d* depicts the H$_2$-TPR profile of the Mn/TiO$_2$. Insignificant H$_2$ consumption at 250–400 °C, according to the literature [41], may be assigned to reduction of Ti^{4+} to Ti^{3+} due to interaction with manganese oxides.
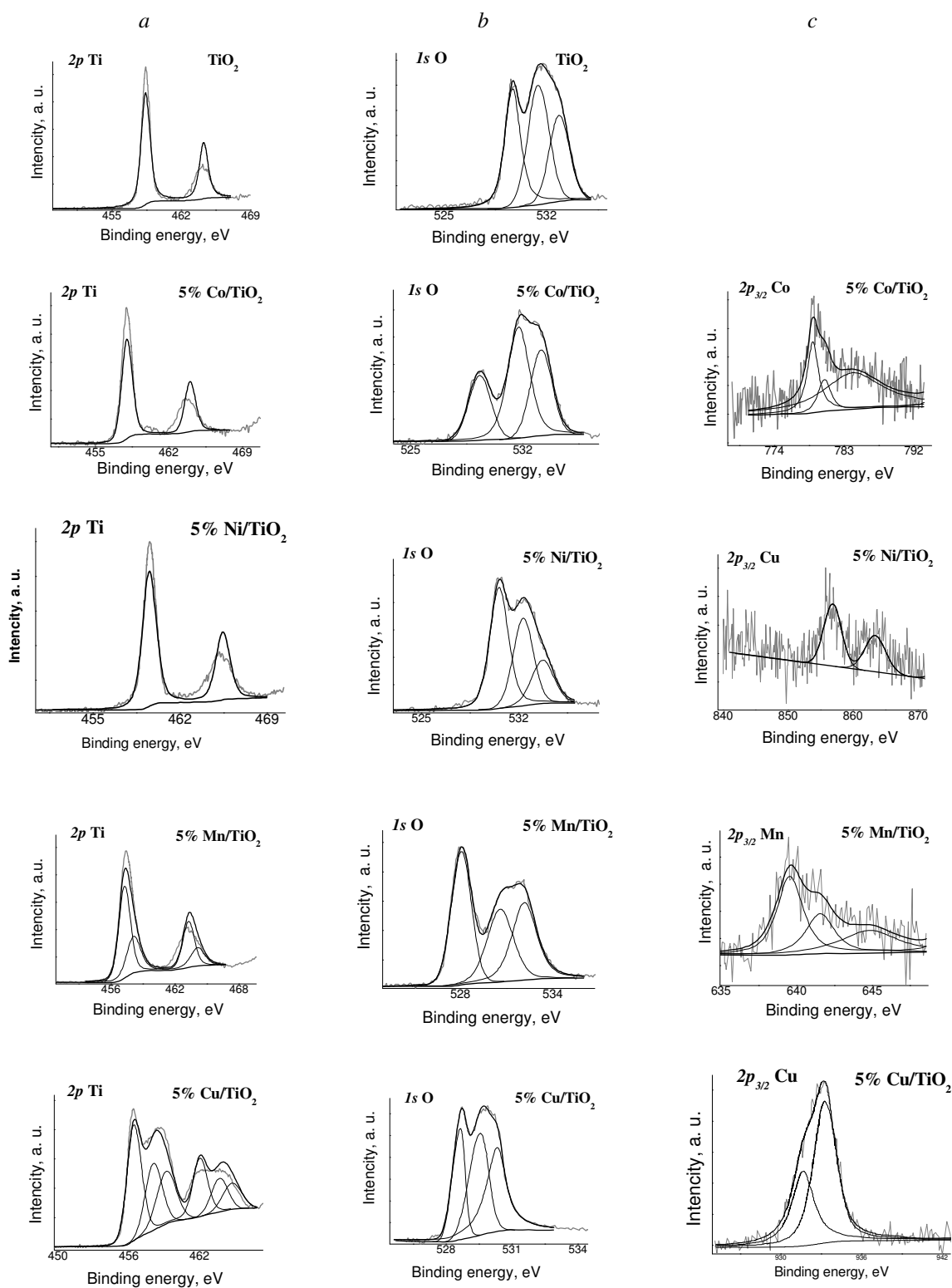

Fig. 2. XPS spectra of TiO$_2$ powders doped with 5 % Co, Ni, Mn, Cu. Binding energy of Ti2*p* - (*a*), O1*s*- (*b*) and 2*p*-electrons of dopant ions (*c*)
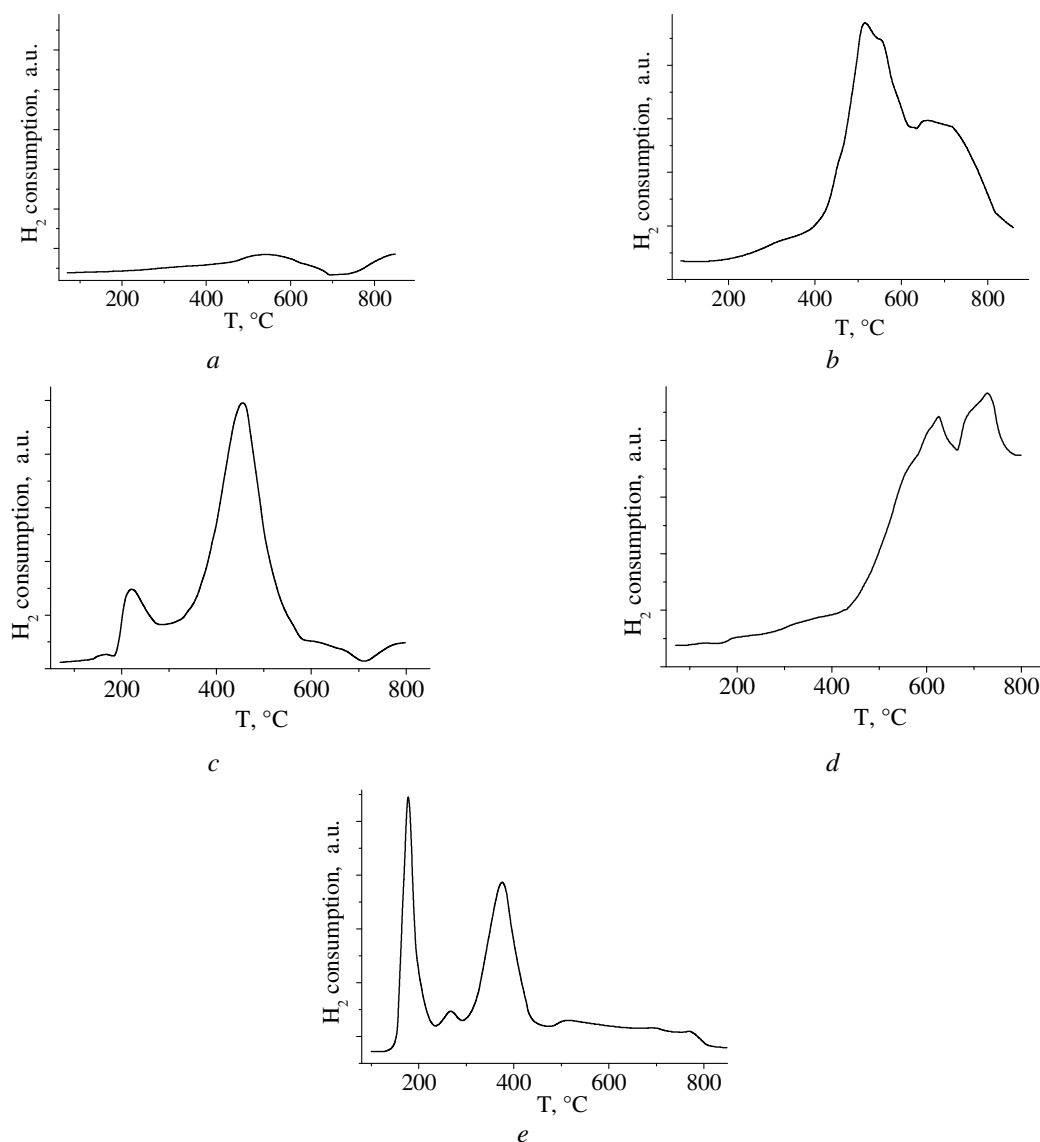
_____

Fig. 3. TPR-profiles of TiO$_2$ and 5 % M^{n+}/TiO$_2$ powders: TiO$_2$ (*a*), Co/TiO$_2$ (*b*), Ni/TiO$_2$ (*c*), Mn/TiO$_2$ (*f*), Cu/TiO$_2$ (*e*)

A broadened appearance of the TPR profile is rather typical for Mn-containing systems, due to an occurrence of manganese species as non-stoichiometric MnO$_x$ oxides. The presence of different oxide species and, consequently, a reduction performance of manganese oxides is influenced by a preparation procedure, quantitative composition and heat treatment conditions [42]. Also, an inherent reducibility of the support plays a great role in a manganese reduction behavior because the support oxide determines the reactivity of the bridging Mn–O–support functionalities.

High-valent ions of transition metals are reduced at lower temperature as compared to low-valent ions. Thus, in accordance with [41–43], a MnO$_2$ reduction process occurs at 250–400 °C.

Since no significant H$_2$ consumption is observed below 450 °C, it can be assumed that noticeable MnO$_2$ amounts have not been formed after the calcination of the Mn/TiO$_2$ at 550 °C in air. It agrees with the reported data [44] about stabilization of low-valence manganese oxide species by support in the systems containing small amounts of manganese. This is in the accordance with the obtained XPS data, where no obvious occurrence of Mn^{4+} was fixed.

Reduction of Mn$_2$O$_3$ to MnO happens according to [42, 43, 46, 47] in the temperature interval of 350–600 °C through the formation of intermediate Mn$_3$O$_4$ in two steps; the temperature ranges are usually 350–500 °C (Mn$_2$O$_3$ → Mn$_3$O$_4$) and 450–600 °C (Mn$_3$O$_4$ → MnO). Thus, two

intense overlapping bands in the TPR profiles with maxima at 650 and 730 °C can are assigned to reduction of Mn_2O_3 to Mn_3O_4 and then to MnO, respectively. However, both processes happened at more high temperature as compared with that in the literature, it is likely to be caused by rather strong interaction between the manganese oxide species and TiO_2.

The TPR profile of Cu/TiO_2 (Fig. 3 *e*) exhibits several reduction peaks. Bulk CuO is known to be reduced at the temperature above 300 °C [47]. But for CuO in composition of $CuO–TiO_2$ systems the reduction of copper species shifts towards low temperatures [50–52]. Due to hydrogen spillover under the reduction conditions, small TiO_2 particles may loose interstitial oxygen and form oxygen deficient TiO_x species. These species are unstable and draw oxygen to form TiO_2 again. Therefore, the CuO matter contacting with them is reduced at relatively low temperature than other CuO particles [51]. Also, taking into account that a sol-gel method stabilizes the CuO phase in a highly dispersed state [49], a peak at 176 °C is ascribed to isolated superficial copper ions or well-dispersed CuO species on the support. A reduction peak centered at 266 °C may be interpreted as a result of reduction isolated Cu^+ ions, their insignificant amount is likely to occur in the Cu/TiO_2 after calcination. A peak with maximum at 375 °C reflects the reduction of large CuO particles. With regard to this temperature, most probably these particles are close to bulk CuO (but their concentration is insufficient for the particles to be detected by XRD).

However, an interpretation of the copper-based catalysts is controversial, because of assumption of some authors [53, 54] about possible realization of stepwise reduction process (i.e. $Cu^{2+} \rightarrow Cu^+$, then $Cu^+ \rightarrow Cu^0$). Proposing the stepwise reduction, the reduction peak at 176 °C can be associated to reduction of isolated Cu^{+2} ions and finely dispersed CuO, in both cases to Cu^{+1}. And the high temperature peak (375 °C) corresponds to a reduction of Cu^{+1} to Cu^0. Also, the temperature of the high-temperature peak (375 °C) coincides that found in the work [54], and it may be indicative of stepwise reduction process.

At the temperature above 500 °C one can observe insignificant hydrogen consumption associated with TiO_2 reduction, which shifts towards low temperatures indicating enhanced reducibility properties of TiO_2 interacting with copper species, in accordance with the literature data [49]. This shift in the reduction temperature of TiO_2 can be explained by presence of Cu^0 clusters (formed after reduction of CuO species) that may catalyze the reduction of Ti^{4+}.

CONCLUSION

• The TPR analysis showed that reduction behaviors of the M^{n+}/TiO_2 were strongly affected by the synthesis method, preparation conditions and interactions between the dopant metal and titanium dioxide matrix.

• Sol-gel synthesis using high concentration of organic components calcinations at 550 °C and applying TiO_2 as a support promoted high-dispersion states of doped 5 % metals, the XPS and TPR showing dopants to exist as divalent and trivalent ions for M^{n+}/TiO_2, where M=Co, Ni, Mn, and as monovalent and divalent ions in the case of Cu/TiO_2.

РФЕС и ТПВ дослідження M/TiO₂ (M=Co, Cu, Mn, Ni) порошків, одержаних золь-гель методом

І.С. Петрик, Г.В. Крилова, О.О. Келип, Л.В. Луценко, Н.П. Смірнова, Л.П. Олексенко

*Інститут хімії поверхні ім. О.О. Чуйка Національної академії наук України
вул. Генерала Наумова, 17, Київ, 03164, Україна, irinapetrik@ukr.net
Київський національний університет імені Тараса Шевченка
вул. Володимирська, 60, Київ, 01601, Україна
University of Notre Dame
132 Nieuwland Science Hall, Notre Dame, IN, 46556*

Одержані темплатним золь-гель методом мезопористі нанорозмірні порошки діоксиду титану, модифікованого йонами 3d металів, досліджені методами РФЕС и ТПВ. Встановлено валентний стан йонів металів на поверхні діоксиду титану. Аналіз термопрограмованого відновлення воднем показав, що відновлювальна здатність M^{n+}/TiO_2 залежить від методу синтезу та умов термообробки. Показано, що формування Ti–O–M зв'язків при золь-гель синтезі, присутність нейонного триблоккополімера Pluronic P123 як органічного темплату та термообробка при 550 °C стабілізують високодисперсний стан металовмісних сполук. Методами РФЕС та ТПВ показано співіснування дво та тривалентних йонів металів для M^{n+}/TiO_2, де M=Co, Ni, Mn, та моно- і дивалентного стану у випадку Cu/TiO₂.

Ключові слова: мезопористі M^{n+}/TiO_2 порошки, Co^{n+}, Ni^{n+}, Mn^{n+} та Cu^{n+} перехідні метали, РФЕС, H_2-ТПВ

РФЭС и ТПВ исследование M/TiO₂ (M=Co, Cu, Mn, Ni) порошков, полученных золь-гель методом

И.С. Петрик, Г.В. Крылова, А.А. Келип, Л.В. Луценко, Н.П. Смирнова, Л.П. Олексенко

*Институт химии поверхности им. А.А. Чуйко Национальной академии наук Украины
ул. Генерала Наумова, 17, Киев, 03164, Украина, irinapetrik@ukr.net
Киевский национальный университет имени Тараса Шевченко
ул. Владимирская, 60, Киев, 01601, Украина
University of Notre Dame
132 Nieuwland Science Hall, Notre Dame, IN, 46556*

Полученные темплатным золь-гель методом мезопористые наноразмерные порошки диоксида титана, модифицированного ионами 3d металлов, изучены методами РФЭС и ТПВ. Установлено валентное состояние ионов металлов на поверхности диоксида титана. Анализ термопрограмированного восстановления водородом показал, что восстановительные способности M^{n+}/TiO_2 зависят от метода получения и условий термообработки. Показано, что формирование связей Ti–O–M при золь-гель синтезе, присутствие неионного триблоксополимера Pluronic P123 как органического темплата и термообработка при 550 °C стабилизируют высокодисперсное состояние металлсодержащих соединений. Методами РФЭС и ТПВ показано сосуществование двух- и трехвалентных ионов металлов для M^{n+}/TiO_2, где M=Co, Ni, Mn, и моно- и дивалентного состоянии в случае Cu/TiO₂.

Ключевые слова: мезопористые M^{n+}/TiO_2 порошки, Co^{n+}, Ni^{n+}, Mn^{n+} и Cu^{n+} переходные металлы, РФЭС, H_2-ТПВ

REFERENCES

1. *Umebayashi T., Yamaki T., Itoh H., Asai K.* Analysis of electronic structures of 3*d* transition metal-doped TiO$_2$ based on band calculations, J. Phys. Chem. Solids, 63 (2002) 1909.

2. *Carp O., Huisman C.L., Reller A.* Photo-induced reactivity of titanium dioxide, Progress in Solid State Chemistry, 32 (2004) 33.

3. *Ghasemi S., Rahimnejad S., Rahman Setayesh S. et al.* Transition metal ions effect on the properties and photocatalytic activity of nanocrystalline TiO$_2$ prepared in an ionic liquid, J. Hazard. Mater., 172 (2009) 1573.

4. *López R., Gómez R., Lianos M.E.* Photophysical and photocatalytical properties of nanosized copper-doped titania sol-gel catalysts, Catal. Today., 148 (2009) 103.

5. *Gomathi Devi L., Girish Kumar S.* Influence of physicochemical–electronic properties of transition metal ion doped polycrystalline titania on the photocatalytic degradation of Indigo Carmine and 4-nitrophenol under UV/solar light, Applied Surface Science, 257 (2011) 2779.

6. *Kim H.-J., Lu L., Kim J.-H. et al.* UV Light induced photocatalytic degradation of cyanides in aqueous solution over modified TiO$_2$, Bull. Korean Chem. Soc., 22 (2001) 1371.

7. *Navío J.A., Juan J.T., Djedjeian P., Padrón J.R. et al.* Iron-doped titania powders prepared by a sol-gel method. Part II: Photocatalytic properties, Appl. Catal. A, 178 (1999) 191.

8. *Zhang F., Jin R., Chen J., Shao C. et al.* High photocatalytic activity and selectivity for nitrogen in nitrate reduction on Ag/TiO$_2$ catalyst with fine silver clusters, J. Catal., 232 (2005) 424.

9. *Sá J., Agüiera C. A., Gross S., Anderson J.A.* Photocatalytic nitrate reduction over metal modified TiO$_2$, Appl. Catal. B, 85 (2009) 192.

10. *Kelyp A.A., Petrik I.S., Losovsky A.V. et al.* Synthesis of photocatalytically active dispersions TiO$_2$/M^{n+} (M=Co, Ni, Mn, Cu) for denitrification of water, Nanosystems, Nanomaterials, Nanotechnologies, 10 (2012) 789.

11. *Suriye K., Praserthdam P., Jongsomjit B.* Effect of surface sites of TiO$_2$ support on the formation of cobalt-support compound in Co/TiO$_2$ catalysts, Catal. Comm., 8 (2007) 1772.

12. *Duvenhage D.J., Coville N.J.* Fe:Co/TiO$_2$ bimetallic catalysts for the Fischer–Tropsch reaction Part 2. The effect of calcination and reduction temperature, Appl. Catal. A, 233 (2002) 63.

13. *Coville N.J., Li J.* Effect of boron source on the catalyst reducibility and Fischer–Tropsch synthesis activity of Co/TiO$_2$ catalysts, Catal. Today, 71 (2002) 403.

14. *Kelyp A.A., Smirnova N.P., Oleksenko L.P. et al.* Catalytic activity of Co/SiO$_2$ and Co/TiO$_2$ nanosized systems in the oxidation of carbon monoxide, Russian Journal of Physical Chemistry A, 87 (2013) 1015.

15. *Petrik I., Kelyp O., Vorobets V. et al.* Synthesis, optical, electro- and photocatalytic properties of nanosized TiO$_2$- films modified with transition metal (Co, Ni, Mn, Cu) ions, Chemistry, Physics and Technology of Surface, 2 (2011) 418.

16. *Kelyp O., Petrik I., Vorobets V. et al.* Sol-gel synthesis and characterization of mesoporous TiO$_2$ modified with transition metal ions (Co, Ni, Mn, Cu), Chemistry, Physics and Technology of Surface, 4 (2013) 105.

17. *Krylova G.V., Gnatyuk Yu.I., Eremenko A.M. et al.* Ag nanoparticles deposited onto silica, titania and zirconia mesoporous films synthesized by sol-gel template method, J. Sol-Gel Sci. Technol., 50 (2009) 216.

18. *Garbassi F., Balducci L.* Preparation and characterization of spherical TiO$_2$-SiO$_2$ particles, Micropor. Mesopor. Mater., 47 (2001) 51.

19. *Keränen J., Guimon C., Iiskola E. et al.* Atomic layer deposition and surface characterization of highly dispersed titania/silica-supported vanadia catalysts, Catal. Today, 78 (2003) 149.

20. *Wagner C.D., Moulder J.F., Davis L.E., Riggs W.M.* Handbook of X-ray Photoelectron Spectroscopy, Perkin-Elmer Corp.: New York, 1979, 671p.

21. *Nefedov V.I.* Roentgenelectronic spectroscopy of chemical compounds: Handbook., Moscow: Khimija, 1984, 255 p. (In Russian).

22. *Nowitzki T., Carlsson A.F., Martyanov O. et al.* Oxidation of alumina-supported Co and Co–Pd model catalysts for the Fischer-Tropsch reaction, J. Phys. Chem. C, 111 (2007) 8566.

23. *Jeong B.-S., Heo Y.W., Norton D.P.* Spatial distribution and electronic state of Co in epitaxial anatase $Co_xTi_{1-x}O_2$ thin films grown by reactive sputtering, Appl. Phys. Lett., 84 (2004) 2608.

24. *Guo Q., Liu Yu.* MnO_x modified Co_3O_4-CeO_2 catalysts for the preferential oxidation of CO in H_2-rich gases, Appl. Catal. B, 82 (2008) 19.

25. *Chu W., Chernavskii P.A., Gengembre L. et al.* Cobalt species in promoted cobalt-alumina-supported Fischer-Tropsch catalysts, J. Catal., 252 (2007) 215.

26. *Berenguer R., Valdes-Solis T., Fuertes A.B. et al.* Cyanide and phenol oxidation on nanostructured Co_3O_4 electrodes prepared by different methods, J. Electrochem. Soc., 155 (2008) 1.

27. *Barakat M.A., Hayes G., Shan S.I.* Effect of cobalt doping on the phase transformation of TiO_2 nanoparticles, J. Nanosci. and Nanotech., 10 (2005) 1.

28. *Tang Q., Zhang Q., Wang P. et al.* Characteristics of cobalt oxide nanoparticles within faujasite zeolites and the formation of metallic cobalt, Chem. Mater., 16 (2004) 1967.

29. *Chupin C., van Veen A.C., Konduru M. et al.* Identity and location of active species for NO reduction by CH over Co-ZSM-5, J. Catal., 241 (2006) 103.

30. *Feng Y., Li L., Niu Sh.et al.* Controlled synthesis of highly active mesoporous Co_3O_4 polycrystals for low temperature CO oxidation, Appl. Catal. B, 111–112 (2012) 461.

31. *Rizhi Ch., Yan D., Weihong X., Nanping X.* The effect of titania structure on Ni/TiO_2 catalysts for *p*-nitrophenol hydrogenation, Chinese J. Chem. Eng., 14 (2006) 665.

32. *Wu Y., He Y., Chen T. et al.* Low temperature catalytic performance of nanosized Ti–Ni–O for oxidative dehydrogenation of propane to propene, Appl. Surf. Sci., 252 (2006) 5220.

33. *Hoffer B.W., van Langeveld A.D., Janssens J.-P. et al.* Stability of highly dispersed Ni/Al_2O_3 catalysts: effect of pretreatment, J. Catal., 192 (2000) 432.

34. *Kantcheva M., Kucukkal M.U., Suzer S.* Spectroscopic investigation of species arising from CO chemisorrption on titania-supported manganese, J. Catal., 190 (2000) 144.

35. *Luo, J.-Y., Meng M., Li X. et al.* Mesoporous Co_3O_4–CeO_2 and Pd/Co_3O_4–CeO_2 catalysts: Synthesis, characterization and mechanistic study of their catalytic properties for low-

36. *Oliveira H.A., Franceschini D.F., Passos F.B.* Support Effect on Carbon nanotube growth by methane chemical vapor deposition on cobalt catalysts, J. Braz. Chem. Soc., 23 (2012) 868.

37. *Tang Ch.-W., Wang Ch.-B., Chien Sh.-H.* Characterization of cobalt oxides studied by FT-IR, Raman, TPR and TG-MS, Thermochimica Acta., 473 (2008) 68.

38. *Wang C.-B., Tang C.-W., Tsai H.-Ch, Chien Sh.-H.* Characterization and catalytic oxidation of carbon monoxide over supported cobalt catalysts, Catal. Lett., 107 (2006) 223.

39. *Morales F., de Groot F.M.F., Gijzeman O.L.J. et al.* Mn promotion effects in Co/TiO_2 Fischer–Tropsch catalysts as investigated by XPS and STEM-EELS, J. Catal., 230 (2005) 301.

40. *Loc L.C., Huan Ng.M., Dung Ng.K. et al.* Study on methanation of carbon monoxide over catalysts NiO/TiO_2 and NiO/γ-Al_2O_3, Adv. Natural Sci., 7 (2006) 91.

41. *Ettireddy P., Ettireddy N., Mamedov S. et al.* Surface characterization studies of TiO_2 supported manganese oxide catalysts for low temperature SCR of NO with NH_3, Appl. Catal. B, 76 (2007) 123.

42. *Derylo-Marczewska A., Gac W., Popivnyak N. et al.* The influence of preparation method on the structure and redox properties of mesoporous Mn-MCM-41 materials, Catal. Today, 114 (2006) 293.

43. *Liang S., Teng F, Bulgan G. et al.* Effect of phase structure of MnO_2 nanorod catalyst on the activity for CO oxidation, J. Phys. Chem. C, 112 (2008) 5307.

44. *Wang. Y., Song Z., Ma D. et al.* Characterization of Rh-based catalysts with EPR, TPR, IR and XPS, J. Mol. Catal. A, 149 (1997) 51.

45. *Park E., Le H.A., Kim Ye.S. et al.* Preparation and characterization of Mn_2O_3/TiO_2 nanomaterials synthesized by combination of CMC and impregnation method with different Mn loading concentration, Mater. Res. Bull., 47 (2012) 1040.

46. *Tang X., Li J., Suna L, Hao J.* Origination of N_2O from NO reduction by NH_3 over β-MnO_2 and α-Mn_2O_3, Appl. Catal. B, 99 (2010) 156.

47. *Zou H., Dong X., Lin W.* CO Selective oxidation in hydrogen-rich gas over copper-

_____

series Catalysts, J. Natural Gas Chem., 14 (2005) 29.

48. *Chen Ch.-Sh., You Y.-H., Lin J.-H., Chen Yu.-Yu.* Effect of highly dispersed active sites of Cu/TiO₂ catalyst on CO oxidation, Catal. Comm., 9 (2008) 2381.

49. *Cordoba G., Viniegra M., Fierro J.L.G. et al.* TPR, ESR, and XPS study of Cu^{2+} ions in sol-gel–derived TiO₂, J. Solid State Chem., 138 (1998) 1.

50. *Li K., Wang Ya., Wang Sh. Et al.* A comparative study of CuO/TiO₂-SnO₂, CuO/TiO₂, and CuO/SnO₂ for methanol dehydrogenation, J. Natural Gas Chem., 18 (2009) 1.

51. *Rong Zh., Yuhan S., Shaoyi P.* Comparative study of Cu/TiO₂ and Cu/ZrO₂ for methanol

dehydrogenation, J. Natural Gas Chem., 9 (2000) 110.

52. *Coloma F., Marquez F., Rochester C.H., Anderson J.A.* Determination of the nature and reactivity of copper sites in Cu-TiO₂ catalysts, Phys. Chem. Chem. Phys., 2 (2000) 5320.

53. *Guerreiro E.D., Gorriz O.F., Rivarola J.B., Arrua L.A.* Characterization of Cu/SiO₂ catalysts prepared by ion exchange for methanol dehydrogenation, Appl. Catal. A., 165 (1997) 259.

54. *Urquieta-Gonzalez E.A., Martins L., Peguin R.P.S., Batista M.S.* Identification of extra-framework species on Fe/ZSM-5 and Cu/ZSM-5 catalysts typical microporous molecular sieves with zeolitic structure, Materials Research., 5 (2002) 321.